Inorg. Chem. **2006**, *45*, 7947–7954

Prediction of pK_a Values of *nido*-Carboranes by Density Functional Theory Methods

Pau Farràs,[†,‡] Francesc Teixidor,*[,‡] and Vicenç Branchadell*[,§]

Institut de Ciència de Materials de Barcelona, CSIC, and Department de Química, Universitat Autònoma de Barcelona, E-08193 Bellaterra, Spain

Received May 24, 2006

A great parallel exists between metal complexes of cyclopentadienyl and arene ligands on one side and metal complexes of the nido derivatives of the icosahedral *o*-carborane clusters. With few exceptions, the metal complexation in the cluster can be viewed as the substitution of one or more bridging hydrogen atoms by the metal. Therefore, a necessary requirement for the complexation is the deprotonation of the nido cluster to generate a coordination site for that metal. The reaction to remove these protons, which most probably is one of the most commonly done processes in boron and metallaborane chemistry, is barely known, and no quantitative data are available on the magnitude of their pK_a values. With the purpose of determining the acidity of *nido*-carboranes, a procedure to calculate the pK_a values of nido boron clusters is presented in this paper for the first time. To this objective, some nido clusters have been selected and their geometry and NMR-spectroscopic properties have been studied, giving a good correlation between the theoretical and experimental data in both geometry distances and ^{11}B NMR spectroscopy. Of notice is the result that proves that the singular carbon atom in the thermodynamic isomer of $[C_2B_{10}H_{13}]^-$ is definitely part of the cluster and that its connection with the C_2B_3 face would be better defined by adding additional interactions with the two boron atoms nearest to the second cluster carbon. The pK_a values of the nido species have been calculated by correlating experimental pK_a values and calculated reaction Gibbs energies ΔG_s. Some pK_a values of importance are −4.6 and +13.5 for 7,8-$[C_2B_9H_{13}]$ (**1**) and 7,8-$[C_2B_9H_{12}]^-$ (**2**), respectively.

1. Introduction

The characteristic feature of carboranes is a triangular-face polyhedral or polyhedral fragment framework of carbon and boron atoms. Prefix designations indicate the degree of "closed" or "open" deltahedral character, with "closo" being a closed deltahedra, "nido" a deltahedral fragment minus a vertex, and "arachno" a deltahedral fragment minus two vertexes. Carboranes follow electron counting rules developed by Mingos,[1] Wade,[2,3] Williams,[4,5] and Rudolph[6,7] that provide an empirical way for predicting the structure of cluster molecules. The polyhedron numbering is illustrated in Figure 1 for the three kinds of boron clusters studied in this work. The boron and carbon atoms are located at the polyhedron vertexes. A terminal hydrogen atom or *exo*-hydrogen is bonded to the cluster's vertex via a classical two-center, two-electron bond. Hydrogen atoms bound intimately to the cluster and whose projection to the cluster's open face falls within its limits are termed *endo*-hydrogen atoms. Also belonging to this type are the hydrogen atoms placed in the surface spanned by the cluster atoms.

nido-Carborane derivatives are key compounds for the coordination of boron clusters with metal ions in the formation of complexes.[8−11] With few exceptions,[12,13] the metal complexation or metal insertion in the cluster can be viewed

* To whom correspondence should be addressed. E-mail: teixidor@icmab.es (F.T.), vicenc.branchadell@uab.es (V.B.).
† P.F. is enrolled in the Ph.D. program at Universitat Autònoma de Barcelona.
‡ Institut de Ciència de Materials de Barcelona, CSIC.
§ Department de Química.

(1) Mingos, D. M. P. *Nature (London), Phys. Sci.* **1972**, *236*, 99.
(2) Wade, K. *J. Chem. Soc. D* **1971**, 792.
(3) Wade, K. *Adv. Inorg. Chem. Radiochem.* **1976**, *18*, 1.
(4) Williams, R. E. *Inorg. Chem.* **1971**, *10*, 210.
(5) Williams, R. E. *Adv. Inorg. Chem. Radiochem.* **1976**, *18*, 67.
(6) Rudolph, R. W.; Pretzer, W. R. *Inorg. Chem.* **1972**, *11*, 1974.
(7) Rudolph, R. W. *Acc. Chem. Res.* **1976**, *9*, 446.
(8) Hawthorne, M. F.; Young, D. C.; Wegner, P. A. *J. Am. Chem. Soc.* **1965**, *87*, 1818.
(9) Zalkin, A.; Templeton, D. H.; Hawthorne, M. F. *J. Am. Chem. Soc.* **1965**, *87*, 3988.
(10) Llop, J.; Viñas, C.; Teixidor, F.; Sillanpää, R.; Kivekäs, R. *Chem.—Eur. J.* **2005**, *11*, 1939.

10.1021/ic060908b CCC: $33.50
Published on Web 08/25/2006

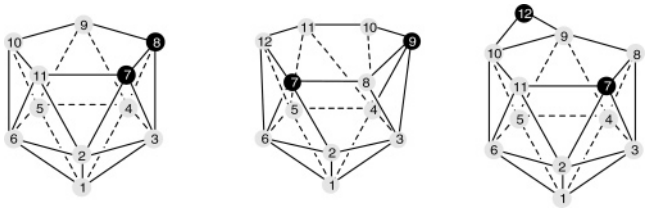

Figure 1. Numbering scheme for nido deltahedral cluster fragments.

as the substitution of one or more bridging hydrogen atoms by the metal. Therefore, a necessary requirement for the complexation is the deprotonation of the nido cluster to generate a coordination site for that metal. The ease of deprotonation is different for each molecule and can be measured by its pK_a value. Experimentally, this can be done by titration or UV spectroscopic measurements. There is, however, little experimental information about the pK_a values of boron clusters[14] because of the difficulty to run on them the methods mentioned above. Therefore, finding a theoretical model to calculate or estimate the pK_a of nido boron clusters will bring relevant information to predicting their behavior. To this objective, some nido clusters have been selected in order to create a procedure that can be used for other *nido*-boranes/carboranes. The studied *nido*-carboranes are shown in Figure 2, also including **2*** for deprotonated **2**.

The binding behavior of the capping hydrogen atoms is shown by studying the geometry and NMR-spectroscopic properties of these molecules. The structure's energy minima found in the gas phase contain the *endo*-hydrogen atoms always bridging two boron atoms. However, there are some molecules in which the bridging hydrogen bounces between two degenerate energy-minimum positions. In these cases, an apparent C_s symmetry is observed in solution by ^{11}B NMR spectroscopy. By analysis of the charge distribution of these compounds, it is demonstrated that the carbon atom on the open face in compound **4**, the thermodynamic $[C_2B_{10}H_{13}]^-$ derivative, is part of the cluster. This had already been discussed, but no proof had been provided. It has also been observed that a clear trend between acidity and molecular charge exists. Thus, neutral compounds are the most acidic, and dianions are the least acidic. This can be proven through the simple model elaborated in this paper to calculate pK_a values of *nido*-carboranes. The procedure is based on a combination of theoretical results and experimental data. Although the matching for **1** with the given experimental value is less than expected, the error for **2** has only been about 0.75 pK_a units.

2. Computational Details

All computations here were carried out with the *Gaussian 98* and *Gaussian 03* packages.[15,16] All geometries were optimized at the B3LYP/6-31G* level[17−21] with no symmetry constraints. Frequency calculations were computed on these geometries at the same level of calculation to verify that they are energy minima. To obtain accurate energies, single-point calculations on the optimized geometries have been performed at the B3LYP/6-311+G** level of theory. Natural population analysis (NPA)[22] charges were also calculated at the B3LYP/6-311+G** level of theory.

^{11}B NMR chemical shifts were calculated at the gauge invariant atomic orbital (GIAO)−B3LYP/6-311+G** level. They have been referenced to B_2H_6 (16.6 ppm)[23] and converted to the usual $BF_3 \cdot OEt_2$ scale; $\delta(^{11}B) = 100.68 - \sigma(^{11}B)$.

The solvation free energy was calculated with either the IPCM (static isodensity polarized continuum model)[24] or the CPCM (conductor polarized continuum model).[25] Dielectric constant values of 78.39 for water and 46.45 for dimethyl sulfoxide (DMSO) were used. In the CPCM model, both UA0 and Bondi radii[26] were used. The Gibbs reaction energies in solution have been computed at 1 mol·L^{-1} and 298.15 K.

3. Results and Discussion

Cluster Geometries and Relative Stabilities of Selected Compounds. Geometry optimizations of the targeted compounds are the first calculations that have to be done in order to get the structure with the minimal energy. This is the starting point from which most of the properties of the molecule can be calculated. A comparison between the X-ray experimental data and theoretical interatomic distances of selected bonds is shown in Table 1.

(11) Núñez, R.; Tutusaus, O.; Teixidor, F.; Viñas, C.; Sillanpää, R.; Kivekäs, R. *Chem.*−*Eur. J.* **2005**, *11*, 5637.
(12) Tutusaus, O.; Viñas, C.; Kivekäs, R.; Sillanpää, R.; Teixidor, F. *Chem. Commun.* **2003**, *19*, 2458.
(13) Teixidor, F.; Flores, M. A.; Viñas, C.; Sillanpää, R.; Kivekäs, R. *J. Am. Chem. Soc.* **2000**, *122*, 1963.
(14) Hlatky, G. G.; Crowther, D. J. *Inorg. Synth.* **1998**, *32*, 229.
(15) Frisch, M. J.; Trucks, G. W.; Schlegel, H. B.; Scuseria, G. E.; Robb, M. A.; Cheeseman, J. R.; Zakrzewski, V. G.; Montgomery, J. A.; Stratmann, R. E.; Burant, J. C.; Dapprich, S.; Millam, J. M.; Daniels, A. D.; Kudin, K. N.; Strain, M. C.; Farkas, O.; Tomasi, J.; Barone, V.; Cossi, M.; Cammi, R.; Mennucci, B.; Pomelli, C.; Adamo, C.; Clifford, S.; Ochterski, J.; Petersson, G. A.; Ayala, P. Y.; Cui, Q.; Morokuma, K.; Malick, D. K.; Rabuck, A. D.; Raghavachari, K.; Foresman, J. B.; Cioslowski, J.; Ortiz, J. V.; Stefanov, B. B.; Liu, G.; Liashenko, A.; Piskorz, P.; Komaromi, I.; Gomperts, R.; Martin, R. L.; Fox, D. J.; Keith, T.; Al-Laham, M. A.; Peng, C. Y.; Nanayakkara, A.; Gonzalez, C.; Challacombe, M.; Gill, P. M. W.; Johnson, B. G.; Chen, W.; Wong, M. W.; Andres, J. L.; Head-Gordon, M.; Replogle, E. S.; Pople, J. A. *Gaussian 98*, revision A.11.3; Gaussian, Inc.: Pittsburgh, PA, 2002.
(16) Frisch, M. J.; Trucks, G. W.; Schlegel, H. B.; Scuseria, G. E.; Robb, M. A.; Cheeseman, J. R.; Montgomery, J. A., Jr.; Vreven, T.; Kudin, K. N.; Burant, J. C.; Millam, J. M.; Iyengar, S. S.; Tomasi, J.; Barone, V.; Mennucci, B.; Cossi, M.; Scalmani, G.; Rega, N.; Petersson, G. A.; Nakatsuji, H.; Hada, M.; Ehara, M.; Toyota, K.; Fukuda, R.; Hasegawa, J.; Ishida, M.; Nakajima, T.; Honda, Y.; Kitao, O.; Nakai, H.; Klene, M.; Li, X.; Knox, J. E.; Hratchian, H. P.; Cross, J. B.; Bakken, V.; Adamo, C.; Jaramillo, J.; Gomperts, R.; Stratmann, R. E.; Yazyev, O.; Austin, A. J.; Cammi, R.; Pomelli, C.; Ochterski, J. W.; Ayala, P. Y.; Morokuma, K.; Voth, G. A.; Salvador, P.; Dannenberg, J. J.; Zakrzewski, V. G.; Dapprich, S.; Daniels, A. D.; Strain, M. C.; Farkas, O.; Malick, D. K.; Rabuck, A. D.; Raghavachari, K.; Foresman, J. B.; Ortiz, J. V.; Cui, Q.; Baboul, A. G.; Clifford, S.; Cioslowski, J.; Stefanov, B. B.; Liu, G.; Liashenko, A.; Piskorz, P.; Komaromi, I.; Martin, R. L.; Fox, D. J.; Keith, T.; Al-Laham, M. A.; Peng, C. Y.; Nanayakkara, A.; Challacombe, M.; Gill, P. M. W.; Johnson, B.; Chen, W.; Wong, M. W.; Gonzalez, C.; Pople, J. A. *Gaussian 03*, revision C.02; Gaussian, Inc.: Wallingford, CT, 2004.
(17) Hariharan, P. A.; Pople, J. A. *Theor. Chim. Acta* **1973**, *28*, 213.
(18) Becke, A. D. *J. Chem. Phys.* **1993**, *98*, 5648.
(19) Lee, C.; Yang, W.; Parr, R. G. *Phys. Rev. B* **1988**, *37*, 785.
(20) Ditchfield, R. *Mol. Phys.* **1974**, *27*, 789.
(21) London, F. *J. Phys. Radium* **1937**, *8*, 397.
(22) Reed, A. E.; Curtiss, L. A.; Weinhold, F. *Chem. Rev.* **1988**, *88*, 899.
(23) Onak, T. P.; Landesman, H. L.; Williams, R. E. *J. Phys. Chem.* **1959**, *63*, 1533.
(24) Foresman, J. B.; Keith, T. A.; Wiberg, K. B.; Snoonian, J.; Frisch, M. J. *J. Phys. Chem.* **1996**, *100*, 16098.
(25) Cossi, M.; Rega, N.; Scalmani, G.; Barone, V. *J. Comput. Chem.* **2003**, *24*, 669.
(26) Bondi, A. *J. Phys. Chem.* **1964**, *68*, 441.

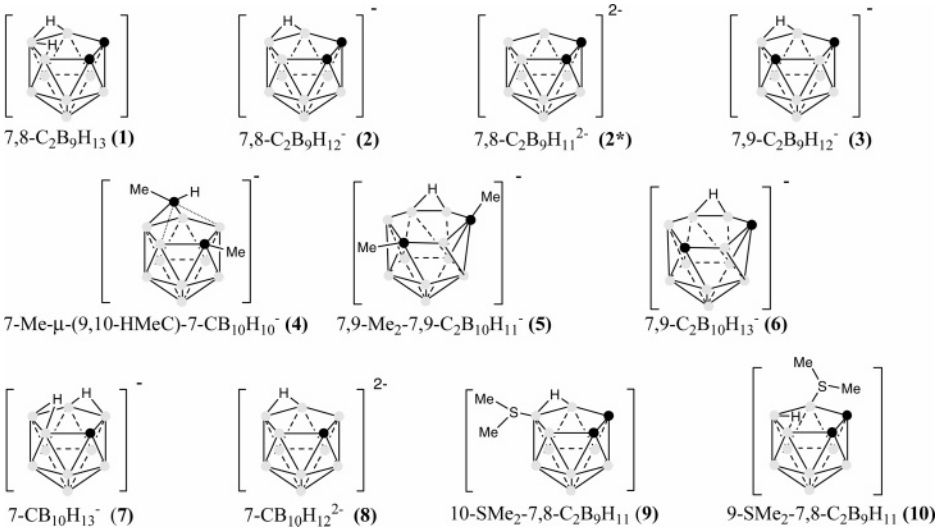

Figure 2. Skeletal structure of studied nido boron clusters. Boron and carbon atoms are shown as light gray and black dots, respectively. *exo*-Hydrogen atoms are not shown.

Table 1. Comparison between the Atom Distances on the Open-Face C_xB_y (Error by the Root-Mean-Square Method)

	2[a]		**3**[b]	
	theor (Å)	exp (Å)	theor (Å)	exp (Å)
C(7)−C(8)	1.557	1.555	1.623	1.625
C(7)−B(11)	1.624	1.607	1.651	1.646
B(11)−B(10)	1.861	1.831	1.851	1.845
B(10)−B(9)	1.882	1.856	1.651	1.641
B(9)−C(8)	1.607	1.614	1.623	1.626
	$R = 0.998$	error = 0.0019	$R = 0.999$	error = 0.0002

	4[c]		**7**[d]	
	theor (Å)	exp (Å)	theor (Å)	exp (Å)
C(7)−B(8)	1.634	1.624	1.648	1.635
C(7)−B(11)	1.634	1.625	1.649	1.640
B(11)−B(10)	1.875	1.867	1.871	1.860
B(10)−C(9)	1.870	1.843	1.905	1.870
B(9)−C(8)	1.875	1.864	1.871	1.851
	$R = 0.998$	error = 0.0011	$R = 0.999$	error = 0.0003

	9[e]		**10**[f]	
	theor (Å)	exp (Å)	theor (Å)	exp (Å)
C(7)−B(8)	1.559	1.547	1.542	1.525
C(7)−B(11)	1.619	1.613	1.601	1.571
B(11)−B(10)	1.852	1.852	1.769	1.775
B(10)−C(9)	1.780	1.792	1.868	1.844
B(9)−C(8)	1.610	1.597	1.646	1.622
	$R = 0.998$	error = 0.002	$R = 0.999$	error = 0.0005

	5[g]	
	theor (Å)	exp (Å)
C(7)−B(8)	1.521	1.506
C(7)−B(12)	1.512	1.513
B(12)−B(11)	1.886	1.885
B(11)−B(10)	1.851	1.846
B(10)−C(9)	1.653	1.648
C(9)−B(8)	1.644	1.638
	$R = 0.999$	error = 0.0003

[a] Experimental data from ref 54. [b] Reference 28. [c] Reference 55. [d] Reference 56. [e] Reference 57. [f] Reference 58. [g] Reference 59.

The relaxed molecular structures of the *nido*-carboranes display considerable deviation from those of the *closo*-carboranes, in which the C−C bond length in *o*-carborane is 1.61 Å, the C−B bonds lie in the range 1.70−1.72 Å, and the B−B bonds lie in the range 1.77−1.79 Å.[38] These parameters are considerably different in the nido species. Therefore, it is clear that removal of the boron atom adjacent to both carbon atoms in *o*-carborane causes a large distortion in the geometry. For example, the two *nido*-carboranes originating from *o*-carborane after formal abstraction of one boron atom, [7,8-$C_2B_9H_{13}$] and [7,8-$C_2B_9H_{12}$]$^-$, display a C−C bond length in the range 1.53−1.55 Å, a C−B bond length of 1.60−1.66 Å, and B−B bonds in the range 1.76−1.89 Å. These changes may be a consequence of a ring current generated in the open face of the nido cluster.

Some of the molecules studied here have already been structurally presented by different authors. This is not the case for compounds **9** and **10**, which had not previously been studied theoretically. The presence of the sulfonium group leads to zwitterionic species. It could be hypothesized that the cluster structural parameters would vary with the sulfonium group. This is not the case, however, because the B−B bond length on the open face is altered only for those bonds incorporating the boron atom bonded to the sulfonium group, producing a bond shortening from 1.88 Å to 1.78 Å in **9** and from 1.86 Å to 1.77 Å in **10**. Moreover, the bond lengths within the cluster are basically equal for both isomers, except those that involve the boron−sulfonium moiety. A comparison between the calculated cage geometries and experimental data shows a good agreement, as seen in Table 2. Experimental C−C distances from X-ray crystallographic investigations for **9** and **10** lie in the range 1.52−1.54 Å, C−B distances in the range 1.57−1.71 Å, and B−B distances in the range 1.72−1.85 Å.

Theoretical structural parameters from this study are as follows: for C−C, 1.54−1.56 Å; for C−B, 1.60−1.74 Å; for B−B, 1.74−1.85 Å. When the *endo*-hydrogen may adopt a bridging or an endo terminal disposition, the bridging disposition is preferred. When compound **9** is symmetrized to C_s symmetry, the energy increases by 15.7 kcal·mol^{-1}, clearly indicating that an nonbridging *endo*-hydrogen is less stable than a bridging hydrogen. The difference in energy

Table 2. Resulting NPA Charges for the Targeted Compounds

	1	2	2*	3	4	5
C(7)	−0.503	−0.577	−0.58	−0.805	−0.728	−0.637
C(8)	−0.503	−0.543	−0.58			
C(9)				−0.805		−0.701
C(12)					−0.501	
B(1)	−0.208	−0.213	−0.243	−0.213	−0.159	−0.203
B(2)	0.039	−0.01	−0.053	−0.022	0.007	0.085
B(3)	0.141	0.127	0.099	−0.022	0.007	0.017
B(4)	0.039	−0.044	−0.053	0.039	−0.231	0.026
B(5)	−0.13	−0.159	−0.184	−0.209	−0.117	−0.214
B(6)	−0.13	−0.184	−0.184	0.039	−0.231	−0.214
B(8)				0.202	0.255	0.325
B(9)	−0.104	−0.018	−0.086		−0.064	
B(10)	−0.125	−0.298	−0.343	−0.035	−0.064	0.08
B(11)	−0.104	−0.01	−0.086	−0.035	0.255	−0.224
B(12)						0.137
H on C	0.274	0.240−0.242	0.21	0.248	0.22	
H on B	0.050−0.202	0.003−0.200	−0.034 to +0.013	−0.007 to +0.156	−0.012 to +0.049	−0.024 to +0.181

	6	7	8	9	10
C(7)	−0.803	−0.801	−0.786	−0.551	−0.562
C(8)				−0.561	−0.529
C(9)	−0.842				
C(12)					
B(1)	−0.207	−0.183	−0.219	−0.197	−0.2
B(2)	0.073	0.014	−0.031	−0.051	0.003
B(3)	0.013	0.014	−0.031	−0.155	0.14
B(4)	0.011	−0.208	−0.19	−0.169	−0.027
B(5)	−0.217	−0.178	−0.183	0.011	−0.144
B(6)	−0.213	−0.208	−0.19	0.142	−0.196
B(8)	0.322	0.019	−0.076		
B(9)		−0.194	−0.285	0.014	−0.037
B(10)	0.064	−0.194	−0.284	−0.282	−0.255
B(11)	−0.223	0.019	−0.077	−0.019	−0.009
B(12)	0.118				
H on C	0.229−0.259	0.25	0.217	0.266	0.264
H on B	−0.030 to +0.180	0.019−0.156	−0.030 to +0.200	0.040−0.195	0.027−0.198

between positional isomers **9** and **10** is 9.1 kcal·mol^{-1}, with **9** being the most stable one.

Concerning **1**−**8** already studied by other authors, our results are in good agreement with theirs.[27−31] Compounds **1**−**3** have been studied using either MP2 or B3LYP methods. If carbon positional isomers **2** and **3** are compared, it is observed that **3** is the most stable by 16.8 kcal·mol^{-1}, similar to the 16.3 kcal·mol^{-1} found in the literature.[27]

For the 12-vertex clusters, two common isomers are known: thermodynamic and kinetic. The former is numbered **4** in this work, whereas the kinetic ones are represented by **5** and **6**. The thermodynamic **4** (with a five-membered face) is the most stable by 3.89 kcal·mol^{-1}, in good agreement with the value found by McKee et al.[32]

Fox et al.[33] have also studied geometrical aspects for the monocarboranes **7** and **8**. As described above, the bridging hydrogen is the most stable of the possible orientations of a capping hydrogen atom and this motif finds its most favorable situation in monocarboranes **7** and **8** for which C_s symmetry instead of C_1 symmetry is possible.

Atomic Charges. This section focuses on the electron distribution in the selected nido compounds. We have analyzed the charge distribution using charges derived from the natural atomic orbital scheme (NPA) because it is known that Mulliken charges are strongly basis set dependent. Calculated NPA charges are shown in Table 2. Trends caused by the difference in electronegativity between carbon and boron atoms, 2.6 and 2.0, respectively, are observed in all compounds. Boron atoms with no carbon neighbors have charges in the range −0.12 to −0.30, those with only one carbon neighbor are in the range +0.14 to −0.11, and those with two carbon neighboring lie between 0.12 and 0.32. The carbon atoms induce an electron flow inside the cluster, causing the boron atoms furthest away from them to be more electron-rich than the other boron atoms. Deprotonation of a *nido*-carborane also changes the electronic distribution in the molecule, especially for the boron atoms that lose the proton and for those occupying their antipodal positions. For example, if Table 2 is inspected, NPA charges on boron atoms B(9,10) and B(2,3) in **2** vary an average of 0.05 units compared with **2*** (**2** deprotonated) as a consequence of losing the bridging hydrogen atom.

Data details in Table 3 indicate that some values are out of the normal range of charges discussed above, and this

(27) Fox, M. A.; Hughes, A. K.; Johnson, A. L.; Paterson, M. A. J. *J. Chem. Soc., Dalton Trans.* **2002**, 2009.
(28) Fox, M. A.; Goeta, A. E.; Hughes, A. K.; Johnson, A. L. *J. Chem. Soc., Dalton Trans.* **2002**, 2132.
(29) Fox, M. A.; Hughes, A. K.; Malget, J. M. *J. Chem. Soc., Dalton Trans.* **2002**, 3505.
(30) Lee, H.; Onak, T.; Jaballas, J.; Tran, U.; Truong, T. U.; To, H. T. *Inorg. Chim. Acta* **1999**, *289*, 11.
(31) Kiani, F. A.; Hofmann, M. *Inorg. Chem.* **2004**, *43*, 8561.
(32) McKee, M. L.; Bühl, M.; Schleyer, P. v. R. *Inorg. Chem.* **1993**, *32*, 1712.
(33) Batsanov, A. S.; Fox, M. A.; Goeta, A. E.; Howard, J. A. K.; Hughes, A. K.; Malget, J. M. *J. Chem. Soc., Dalton Trans.* **2002**, 2624.

Table 3. Summary of Calculated ^{11}B NMR Shifts

compd	formula	calcd ^{11}B NMR chemical shifts (ppm)
1	7,8-$C_2B_9H_{13}$	3.7 (2,4), −3.4 (5,6), −17.3 (3), −20.6 (10), −30.4 (9,11), −31.0 (1)
2	7,8-$C_2B_9H_{12}^-$	−14.6 (9,11), −18.0 (5,6), −20.5 (3), −24.6 (2,4), −35.1 (10), −41.1 (1)
3	7,9-$C_2B_9H_{12}^-$	−6.3 (2,5), −8.3 (8), −23.7 (3,4), −26.8 (10,11), −37.8 (1), −38.3 (6)
4	7-Me-μ-(9,10-HMeC)-7-$CB_{10}H_{10}^-$	16.9 (8,11), 8.4 (5), −1.0 (1), −6.9 (2,3), −14.7 (9,10), −21.6 (4,6)
5	7,9-Me_2−7,9-$C_2B_{10}H_{11}^-$	8.8 (8), 0.8 (10,12), −2.6 (3), −10.9 (5,6), −17.8 (2,4), −21.6 (1), −22.3 (11)
6	7,9-$C_2B_{10}H_{13}^-$	8.7 (8), −0.2 (10,12), −7.1 (3), −9.8 (5,6), −19.6 (1), −21.8 (11), −23.7 (2,4)
7	7-$CB_{10}H_{13}^-$	−1.3 (5), −13.5 (2,3), −15.2 (8,11), −26.2 (9,10), −29.0 (1), −33.6 (4,6)
8	7-$CB_{10}H_{12}^{2-}$	−17.7 (8,11), −18.9 (4,6), −25.7 (2,3), −29.1 (5), −31.8 (9,10), −46.1 (1)
9	10-SMe_2−7,8-$C_2B_9H_{11}$	−15.5 (5,6), −17.3 (9,11), −18.9 (3), −20.6 (2,4), −25.9 (10), −39.5 (1)
10	9-SMe_2−7,8-$C_2B_9H_{11}$	−4.5 (5), −6.3 (9), −12.7 (2), −16.9 (11), −18.6 (3), −23.5 (4), −26.6 (6), −30.3 (10), −37.1 (1)

Table 4. Correlation Coefficients between Theoretical and Experimental ^{11}B NMR Chemical Shifts

	correlation coefficient	
	no symmetry	with apparent symmetry
1[a]	0.997	
2[b]	0.829	0.996
3[c]	0.998	
4[c]	0.996	
5[d]	0.634	0.975
6[c]	0.653	1.000
7[c]	0.997	
8[e,g]	0.945	
9[f]	0.703	0.949
10[c]	0.984	

[a] Experimental data from ref 14. [b] Reference 60. [c] Reference 61. [d] Unpublished results. [e] Reference 33. [f] Reference 62. [g] Not known experimentally. Data from a zwitterionic-based molecule: $[Me_3NCB_{10}H_{11}]^-$.

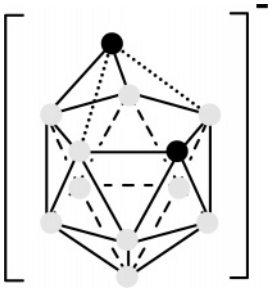

Figure 3. Scheme of B−C interactions in **4**.

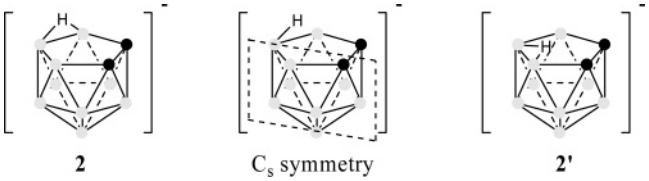

Figure 4. C_s symmetry caused by the fluxional hydrogen atom.

could imply relevant structural information. In this context, NPA charges on B(8,11) in **4** are 0.255, much higher than would be expected for boron atoms bonded to only one carbon. In the common structural representation, these boron atoms are linked to one carbon atom, but their charge is out of the margin of NPA charges expected for a boron atom connected to a carbon and is closer to the value of a boron atom attached to two carbon atoms. Indeed, **4** originates from a *closo*-carborane (*o*-carborane) in which C(12) is attached to both C(7) and B(8,11). Thus, in *o*-carborane, these two boron atoms are bonded to two carbon atoms, and the introduction of two electrons (reduction of the cluster) moves C(12) away from C(7), diminishing the bond order with C(7) and B(8,11) but not to the point of reducing it to zero. We understand that Figure 3 represents more precisely the bonding interaction in **4**.

Using the natural atomic orbitals obtained from the NPA calculation, Wiberg bond orders[34] have been calculated for compound **4**. The Wiberg bond order of the B−C bonds indicated by the dotted lines in Figure 3 is 0.1694, which represents 24.4% of the average value of the remaining B−C bonds in **4** (0.695). This is the first confirmation that the previously known $C_{exo\ cluster}$ [C(12)] is, indeed, part of the cluster because there is additional interaction as shown before with the two remaining boron atoms of the open face.

NMR Calculations. The ultimate goal of this work is to calculate the acidity of the targeted compounds in solution. Thus, it was first necessary to verify if the optimized structures in the gas phase are consistent with the experimental data in solution. NMR gives information on the nature of each nucleus in a liquid environment (a solution). Therefore, if a good correlation between the theoretical and experimental chemical shifts is achieved, then the optimized geometry may be considered a good representation of its molecular structure in solution.[35−38] Because all molecules are boron cages and they are well characterized by ^{11}B NMR spectroscopy, we can use the experimental values obtained with this technique and compare them with the calculated ones. It has already been proven that the GIAO/B3LYP method is suitable for these molecules, and our calculations on compounds **1**−**3** and **6**−**8** are in agreement with previously reported values in the literature at various computational levels.[27−33] A summary of our results is shown in Table 3.

These values can be compared with experimental data. Table 4 shows the corresponding correlation coefficients (*R*). It can be observed that in cases where the position of the fluxional proton can produce C_s symmetry the correlation is very bad. However, if it is considered that apparent C_s symmetry is achieved by a fast interchange of the bridging proton between the two extreme positions shown in Figure 4, then *R* becomes very good indeed. The reason is that these protons have a rapid movement between two positions that corre-

(34) Wiberg, K. B. *Tetrahedron* **1968**, *24*, 1083.
(35) Bühl, M.; Schleyer, P. v. R. *J. Am. Chem. Soc.* **1993**, *114*, 477.
(36) Bühl, M.; Gauss, J.; Hofmann, M.; Schleyer, P. v. R. *J. Am. Chem. Soc.* **1993**, *115*, 12385.
(37) Schleyer, P. v. R.; Gauss, J.; Bühl, M.; Greatrex, R.; Fox, M. A. *J. Chem. Soc., Chem. Commun.* **1993**, 1766.
(38) Fox, M. A.; Greatrex, R.; Hofmann, M.; Schleyer, P. v. R. *J. Organomet. Chem.* **2000**, *614*−*615*, 262.

Table 5. Theoretical Gas-Phase Deprotonation Enthalpies for Carboranes **1**−**10**, Methanol, Trifluoroacetic Acid, and Benzoic Acid[53]

compound	ΔH (kcal·mol^{-1})	compound	ΔH (kcal·mol^{-1})[a]
1	305.32	**8**	534.79
2	438.44	**9**	333.82
3	437.71	**10**	347.95
4	434.35	methanol	384.1 (381.5)
5	427.22	trifluoroacetic acid	321.4 (322.9)
6	429.72	benzoic acid	343.5 (340.1)
7	433.99		

[a] The experimental values in parentheses were taken from ref 53.

sponds to degenerate energy minima, giving as an average a central position with the corresponding C_s symmetry.

The worst correlation coefficient (R) is 0.945 for **8**. This is due to the lack of a experimental structure, this for $[7\text{-}CB_{10}H_{12}]^{2-}$, from which the NMR data could be taken to be compared with the computed structure. The compared NMR data are from $[7\text{-}Me_3N\text{-}7\text{-}CB_{10}H_{11}]^-$ (exp) and $[7\text{-}CB_{10}H_{12}]^{2-}$ (computed). In the case for **9**, the fitting $R = 0.949$ is not too good either. This may be interpreted as if the proton bouncing process and the restricted sulfonium group rotation have dissimilar rates. This results in the fact that the simple apparent C_s symmetry procedure described above does not describe accurately the molecular structure in solution. Besides these two cases, there is a good agreement between the calculated and experimental chemical shifts. Therefore, the assumption that the optimized geometry is representative of the geometry in solution is reasonable.

Gas-Phase Acidity. Because of substantial experimental and theoretical difficulties, well-defined pK_a values of carborane molecules are not available in almost any case. Measurements and calculations on *closo*-carborane isomers have been reported, although their calculation method was at most qualitative.[39] More recently and because of new experimental results, the interest for carborane acidity has grown and gas-phase acidity calculations have been done for *closo*-$CB_{11}H_{12}^-$ and its derivatives showing its strongly acidic properties.[40−45]

Gas-phase deprotonation enthalpies provide valuable information about the inherent solvent-independent properties of acids AH. They correspond to the reaction enthalpy of the gas-phase process

$$AH \rightarrow A^- + H^+$$

The computed deprotonation enthalpies of carboranes **1**−**10** are presented in Table 5 and Figure 5 along with those computed for three organic acids for which experimental values are known.

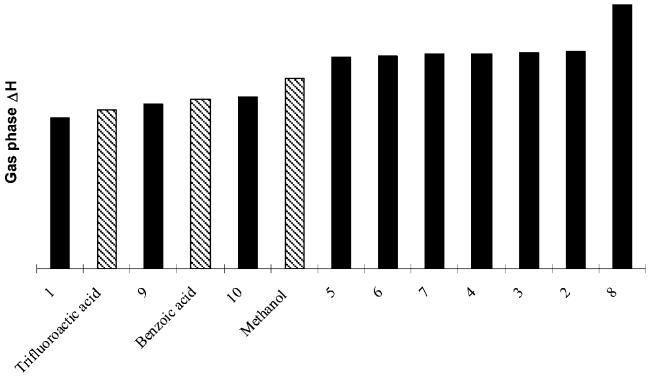

Figure 5. Theoretical gas-phase deprotonation enthalpies (kcal·mol^{-1}) by acidity order.

From Figure 5, three different orders of magnitude of acidity can be observed. Compounds **9** and **10** have a deprotonation energy between 330 and 350 kcal·mol^{-1}, which is in the range of trifluoroacetic acid and benzoic acid. Compound **1** can also be included in this group although its deprotonation energy is lower, 305 kcal·mol^{-1}; thus, it is the strongest acid. Compounds **2**−**7** have $\Delta H = 433 \pm 5$ kcal·mol^{-1} and can be set in a second group. Although these values are higher than that of methanol, 384 kcal·mol^{-1}, we have taken this as a reference and it would be the strongest acid within this group. Within another range of acidity, we encounter compound **8** with $\Delta H = 535$ kcal·mol^{-1}.

A parallel between the deprotonation energy and charge properties of the studied compounds can be found. The most acidic ones are neutral (**1**) or zwitterionic (**9** and **10**); compounds in the second range are monoanions, and the least acidic (**8**) is a dianion. In summary, it is possible to have a first qualitative approximation to the acidity of a nido-targeted compound from its charge.

Solution-Phase Acidity. The pK_a of an acid AH can be computed[46−50] from the reaction Gibbs energy associated with direct deprotonation in solution

$$AH(solv) \rightarrow A^-(solv) + H^+(solv) \qquad (1)$$

or with proton transfer to the conjugate base of a reference acid (BH).

$$AH(solv) + B^-(solv) \rightarrow A^-(solv) + BH(solv) \qquad (2)$$

$$pK_a(AH) = \Delta G_s/2.30RT + pK_a(BH)$$

where ΔG_s = reaction Gibbs energy in solution

This second approach avoids the difficult problem of computing the Gibbs solvation energy of the proton and is the one that we have chosen, using methanol as the reference acid.

(39) Hermansson, K.; Wójcik, M.; Sjöberg, S. *Inorg. Chem.* **1999**, *38*, 6039.
(40) Koppel, I. A.; Burk, P.; Koppel, I.; Leito, I.; Sonoda, T.; Mishima, M. *J. Am. Chem. Soc.* **2000**, *122*, 5114.
(41) Juhasz, M.; Hoffmann, S.; Stoyanov, E. S.; Kim, K.; Reed, C. A. *Angew. Chem., Int. Ed.* **2004**, *43*, 5352.
(42) Reed, C. A. *Chem. Commun.* **2005**, 1669.
(43) Stoyanov, E. S.; Kim, K.; Reed, C. A. *J. Am. Chem. Soc.* **2006**, *128*, 1948.
(44) Stoyanov, E. S.; Hoffmann, S. P.; Juhasz, M.; Reed, C. A. *J. Am. Chem. Soc.* **2006**, *128*, 3160.
(45) Balanarayan, P.; Gadre, S. R. *Inorg. Chem.* **2005**, *44*, 9613.
(46) Klamt, A.; Eckert, F.; Diedenhofen, M. *J. Phys. Chem. A* **2003**, *107*, 9380.
(47) Almerindo, G. I.; Tondo, D. W.; Piego, J. R., Jr. *J. Phys. Chem. A* **2004**, *108*, 166.
(48) Liptak, M. D.; Shields, G. C. *J. Am. Chem. Soc.* **2001**, *123*, 7314.
(49) Magill, A. M.; Cavell, K. J.; Yates, B. F. *J. Am. Chem. Soc.* **2004**, *126*, 8717.
(50) Martin, D.; Illa, O.; Baceiredo, A.; Bertrand, G.; Ortuño, R. M.; Branchadell, V. *J. Org. Chem.* **2005**, *70*, 5671.

Table 6. Comparison of Calculated pK_a Values in Water Using Different Methods According to Equation pK_a = pK_a(exp,MeOH) + ΔG_s/2.303RT

	IPCM[a,b]	CPCM(UA0)[a,b]	CPCM(Bondi)[a,b]	exp
1	−26.8	−23.5	−17.9	2.98
2	10.7	5.6	9.5	14.25

	CPCM/6-311+G(2d,2p)[a,c]	CPCM/CPCM[b,d]
1	−24.2	−20.1
2	7.4	10.9

[a] Geometries optimized in the gas phase at the B3LYP/6-31G* level. [b] Solvation energies computed at the B3LYP/6-311+G** level. [c] Solvation energies computed at the B3LYP/6-311+G(2d,2p) level using UA0 radii. [d] Geometries optimized in solution at the B3LYP/6-31G* level using UA0 radii.

Our initial goal was to compute pK_a values in water; however, the preliminary inconsistent results led us to use DMSO in preference, although studies in water have also been done. The problem with water is that polarizable continuum models for solvation are less accurate in this solvent than in others.[51] Moreover, most of the reactions of *nido*-carboranes are done in organic solvents so data in an organic solvent such as DMSO should be useful for synthetic purposes.

Calculation of the solvation energies for all molecules participating in the reaction can be done by different available continuum methods such as IPCM or CPCM. Both have been used to find the best model that parallels the computed values and the experimental data found in the literature.[14] To choose a suitable method for our compounds, a comparison of the results obtained by the different methods is shown in Table 6 for **1** and **2**. It is clear that the results for **1** are very bad in all cases, whereas for **2**, the best result is obtained by using IPCM. We have also studied the benefits that would generate a more accurate calculation using either a larger basis set to calculate solvation energies of the molecules or the optimization of the molecules in solution. Although results have been improved by optimizing geometries in solution, the calculated value for **2** is still very similar to the one obtained by IPCM. To our understanding, the computational time used by each molecule is so high (4 times more in the optimization) that it does not make the larger cost in computing time worthy. Therefore, IPCM has been selected as the best method available for our calculation. For further information, see the Supporting Information.

To improve the values obtained before, a combination between the experimental and theoretical data is used. The reaction Gibbs energy in solution ΔG_s has been computed for the proton transfer indicated in eq 2 from seven organic acids to MeO^-, and these values have been correlated with the experimental pK_a values. The linear regression leads to the following equations:

$$pK_a = 0.3551\Delta G_s + 15.844 \ (r = 0.98) \qquad \text{for water} \quad (3)$$

$$pK_a = 0.5876\Delta G_s + 29.082 \ (r = 0.99) \qquad \text{for DMSO} \quad (4)$$

(51) Chipman, D. M. *J. Phys. Chem. A* **2002**, *106*, 7413.

Table 7. Calculated ΔG_s (kcal·mol^{-1}) for the Proton Transfer to MeO^- and pK_a Values of Studied Compounds in Water and DMSO

	water		DMSO	
	ΔG_s	pK_a	ΔG_s	pK_a
1	−57.7	−4.6	−57.9	−4.9
2	−6.6	13.5	−6.1	25.5
3	−8.7	12.8	−8.1	24.3
4	−5.8	13.8	−5.2	26.0
5	−12.3	11.5	−11.7	22.2
6	−14.0	10.9	−13.4	21.2
7	−17.6	9.6	−13.6	21.1
8	22.1	23.7	28.5	45.8
9	−30.1	5.2	−30.3	11.3
10	−25.8	6.7	−23.3	15.4

These equations have been used to compute the pK_a values of the targeted molecules from the computed ΔG_s. The results obtained in both water and DMSO are shown in Table 7.

The critical point in calculating pK_a values is the solvation energies of the participating molecules. If for organic molecules good accuracy is difficult to obtain, in *nido*-carboranes, the accuracy would be even worse because of the size of these molecules. The results obtained in water for **1** and **2** can be compared with the experimental values, 2.98 and 14.25, respectively, found in the literature.[14] The discrepancy in **1** is considerable, although it is well-known that experimental pK_a calculation of very acidic compounds is still very difficult, and perhaps the −4.6 value may not be so far from reality. On the contrary, the error for **2** is only 0.75 units of pK_a. Thus, we can consider that the results obtained for the other compounds are good enough and that this procedure may be worth quantitatively calculating pK_a values of *nido*-carboranes, taking the values for very acidic compounds with caution. Therefore, we feel that this procedure provides sufficient accuracy, reliability, and easiness to make it valuable for the calculation of pK_a values of *nido*-carborane anions.

4. Conclusions

Theoretical methods incorporating solvation energy protocols based only on one experimental reference have proven to be unsuccessful in calculating pK_a values of *nido*-carboranes because the computed values are very far from the few experimental data available. More realistic and useful pK_a data have been obtained through the use of a set of acids with well-defined pK_a values, which have made it possible to describe a linear equation relating the pK_a with the reaction Gibbs energy in solution, ΔG_s, in both water and DMSO. From ΔG_s for the studied nido species, it is then possible to calculate the pK_a values. The results obtained compare well with the experimental data available and are consistent with the structures, number of acidic protons, and charges of the species studied. From these, it is then possible to draw some pK_a conclusions: the monoprotic zwitterionic species represented by the sulfonium derivatives **9** and **10** have pK_a values comparable to those of alkyl organic acids; the diprotic neutral species [7,8-$C_2B_9H_{13}$] may be comparable to a trifluoroacetic acid, the monoprotic monoanionic species to pyrrole, and monoanionic diprotic species to phenols. Finally,

the least acidic are the dianionic monoprotic species that compare with *tert*-butyl alcohol/aniline.

In addition to the charge structure/pK_a correlation described here, these studies also suggest that the problem associated with the pK_a calculation derives from the solvation energy. Taking this into account, the extremely good correlation between the calculated and experimental ^{11}B NMR data is remarkable. It is even more so if we consider that energy optimization of the boron clusters is done in the gas phase. This leads to the conclusion that there is, in general, little interaction of these nido species with solvent molecules, in contrast with phosphorus-containing species, which seem to interact strongly.[52]

Acknowledgment. This work was supported, in part, by CICYT (Project MAT2004-01108), Generalitat de Catalunya (Grant 2005/SGR/00709), and CSIC (Grant I3P for P.F.). Access to the computational facilities of Centre de Supercomputació de Catalunya and the CSIC computing center is also gratefully acknowledged.

Supporting Information Available: Table containing computed total energies and Cartesian coordinates for compounds **1**−**10**, tables for computed ΔG_s and pK_a for compounds **1**−**10** and selected acids using different available continuum methods, figures for the linear regressions between theoretical ΔG_s and experimental pK_a using ICPM and CPCM to calculate solvation energies. This material is available free of charge via the Internet at http://pubs.acs.org.

IC060908B

(52) Nuñez, R.; Farras, P.; Teixidor, F.; Viñas, C.; Sillanpää, R.; Kivekäs, R. *Angew. Chem., Int. Ed.* **2006**, *45*, 1270.
(53) Hunter, E. P.; Lias, S. G. In *Proton Affinity Evaluation*; Linstrom, P. J., Mallard, W. G., Eds.; NIST Chemistry WebBook, NIST Standard Reference Database Number 69; National Institute of Standards and Technology: Gaithersburg, MD, June 2005 (http://webbook.nist.gov).
(54) Davidson, M. G.; Fox, M. A.; Hibbert, T. G.; Howard, J. A. K.; Mackinnon, A.; Neretin, I. S.; Wade, K. *Chem. Commun.* **1999**, 1649.
(55) Churchill, M. R.; DeBoer, B. G. *Inorg. Chem.* **1973**, *12*, 2674.
(56) Whitaker, C. R.; Romerosa, A.; Teixidor, F.; Rius, J. *Acta Crystallogr.* **1995**, *C51*, 188.
(57) Tutusaus, O.; Teixixor, F.; Nuñez, R.; Viñas, C.; Sillanpää, R.; Kivekäs, R. *J. Organomet. Chem.* **2002**, *657*, 247.
(58) Cowie, J.; Hamilton, E. J. M.; Laurie, J. C. V.; Welch, A. J. *Acta Crystallogr.* **1988**, *C44*, 1648.
(59) Getman, T. D.; Knobler, C. B.; Hawthorne, M. F. *Inorg. Chem.* **1990**, *29*, 158.
(60) Fontaine, X. L. R.; Greenwood, N. N.; Kennedy, J. D.; Nestor, K.; Thornton-Pett, M.; Hernanek, S.; Jelinek, T.; Stibr, B. *J. Chem. Soc., Dalton Trans.* **1990**, 681.
(61) Plesek, J.; Stibr, B.; Fontaine, X. L. R.; Kennedy, J. D.; Hermanek, S.; Jelinek, T. *Collect. Czech. Chem. Commun.* **1991**, *56*, 1618.
(62) Plesek, J.; Jelinek, T.; Mares, F.; Hermanek, S. *Collect. Czech. Chem. Commun.* **1993**, *58*, 1534.